Available online at www.sciencedirect.com
ScienceDirect
Chemical Geology 247 (2008) 124–132
CHEMICAL GEOLOGY INCLUDING ISOTOPE GEOSCIENCE
www.elsevier.com/locate/chemgeo

Oxidation of pyrite during extraction of carbonate associated sulfate

Pedro J. Marenco [a,*], Frank A. Corsetti [a], Douglas E. Hammond [a], Alan J. Kaufman [b], David J. Bottjer [a]

[a] Department of Earth Sciences, University of Southern California, Los Angeles, CA, 90089-0740, USA
[b] Department of Geology, University of Maryland, College Park, MD, 20742-4211, USA

Received 27 February 2007; received in revised form 10 October 2007; accepted 13 October 2007

Editor: D. Rickard

Abstract

The sulfur isotopic composition of carbonate associated sulfate (CAS) has been used to investigate the geochemistry of ancient seawater sulfate. However, few studies have quantified the reliability of $\delta^{34}S$ of CAS as a seawater sulfate proxy, especially with respect to later diagenetic overprinting. Pyrite, which typically has depleted $\delta^{34}S$ values due to authigenic fractionation associated with bacterial sulfate reduction, is a common constituent of marine sedimentary rocks. The oxidation of pyrite, whether during diagenesis or sample preparation, could thus adversely influence the sulfur isotopic composition of CAS. Here, we report the results of CAS extractions using HCl and acetic acid with samples spiked with varying amounts of pyrite. The results show a very strong linear relationship between the abundance of fine-grained pyrite added to the sample and the resultant abundance and $\delta^{34}S$ value of CAS. This data represents the first unequivocal evidence that pyrite is oxidized during the CAS extraction process. Our mixing models indicate that in samples with much less than 1 wt.% pyrite and relatively high $\delta^{34}S_{pyrite}$ values, the isotopic offset imparted by oxidation of pyrite should be much less than −4‰. A wealth of literature exists on the oxidation of pyrite by Fe^{3+} and we believe this mechanism drives the oxidation of pyrite during CAS extraction, during which the oxygen used to form sulfate is taken from H_2O, not O_2. Consequently, extracting CAS under anaerobic conditions would only slow, but not halt, the oxidation of pyrite. Future studies of CAS should attempt to quantify pyrite abundance and isotopic composition.

Keywords: Carbonate associated sulfate; CAS; $\delta^{34}S$; Pyrite

1. Introduction

The sulfur isotopic composition of seawater sulfate is an important geochemical indicator of changing global redox conditions. In order to investigate the changing oxidation state of surface environments, sulfate-bearing evaporite minerals have traditionally been used to construct broadly-defined $\delta^{34}S$ age curves (e.g., Claypool et al., 1980; Holser, 1984; Canfield, 1998). However, evaporites are less than ideal insofar as they 1) often form in restricted settings, 2) are uncommon in Precambrian rocks, and 3) lack the age diagnostic fossils necessary for precise correlation. The drawbacks to evaporite chemostratigraphy can be overcome by analyzing trace amounts of sulfate

* Corresponding author. University of California at Riverside, Department of Earth Sciences, 1432 Geology, Riverside, CA 92521-0423, USA. Tel.: +1 951 827 3728.
E-mail address: marenco@ucr.edu (P.J. Marenco).

0009-2541/$ - see front matter © 2007 Elsevier B.V. All rights reserved.
doi:10.1016/j.chemgeo.2007.10.006

incorporated into the calcium-carbonate lattice of carbonate minerals (carbonate associated sulfate, CAS) at the time of precipitation (Kaplan et al., 1963; Mekhtiyeva, 1974; Burdett et al., 1989). Carbonates are more ideal than evaporites because they commonly form in normal marine settings, have a broader distribution in time and space, and contain fossils that can be used for precise correlation. CAS has been used to construct $\delta^{34}S$ profiles for the Phanerozoic (Kampschulte and Strauss, 2004) as well as for a number of higher-resolution studies focused on specific transitions in Earth history (Kaiho et al., 2001; Hurtgen et al., 2002; Kah et al., 2004; Newton et al., 2004; Gellatly and Lyons, 2005; Kaiho et al., 2006; Riccardi et al., 2006; Marenco, 2007).

Although the use of CAS has become more widespread, few investigations of the reliability of the method have been published (Lyons et al., 2004; Marenco, 2007). One particular concern regarding the use of CAS is the possibility that pyrite present in whole rock samples would be oxidized to sulfate during the CAS extraction process. To date, a systematic controlled investigation of pyrite oxidation during CAS extraction has not been available. Here, we present unambiguous data that demonstrates the oxidation of pyrite during CAS extraction, using both strong (HCl) and weak (acetic) acids.

2. Methods and material studied

2.1. Geologic setting and previous work

The limestone sample used in this study was collected from the Virgin Limestone Member of the Moenkopi Formation near Lost Cabin Springs in southern Nevada, USA. The Virgin Limestone Member at Lost Cabin Springs was deposited under subtidal marine conditions on a distally-steepened carbonate ramp (Blakey, 1974) during the Spathian Stage of the Early Triassic (McKee, 1954). Isotopic analyses of Spathian evaporites from more onshore facies of the Moenkopi Formation have yielded $\delta^{34}S$ values approaching +30 ‰ CDT (Wilgus, 1981; Marenco, 2007) whereas CAS studies have reported values as high as +38 ‰ (Marenco, 2007).

2.2. CAS extraction using hydrochloric and acetic acid

The limestone sample for isotopic analysis was first prepared by trimming obvious diagenetic phases (e.g., large veins and weathering rinds) and was subsequently powdered using a Rock Labs standard split-discus mill. The homogenized powdered sample was split into eight sub-samples ranging from 135 to 150 g (Table 1), four to be used for CAS extraction using HCl, and four to be used for CAS extraction using CH_3COOH. The samples were then combined with granular pyrite (FeS_2 distributed by EMD, guaranteed 85% pure through 50 mesh) to make a total of 150 g using approximately 0, 1.5, 7.5, and 15 g of pyrite. One set of samples containing 0, 1, 5 and 10% pyrite was used for CAS extraction with HCl and the other set was used for CAS extraction using CH_3COOH.

CAS was extracted via a method modified from Burdett et al. (1989). Samples were subjected to two consecutive eight-hour washes in 1 l of 18.2 MΩ distilled water to dissolve any soluble sulfur phases. After each wash, the fluid was removed. The samples were then washed for eight hours in a solution consisting of 52.5 ml of 6% NaOCl added to 947.5 ml of DDI water to dissolve organic sulfur phases. After removing the fluid from the previous step, the samples were then subjected to two additional washes with DDI water to dilute and remove residual bleach as well as to remove non-CAS-bound sulfur not removed during the previous steps.

Once the sample powders were free of water-soluble sulfur phases, they were dissolved using 3 M HCl or 3 M CH_3COOH. The reaction stoichiometry requires one liter of HCl or CH_3COOH for a 150 g sample, assuming no insolubles and no mass lost during the wash steps. The samples were allowed to dissolve for

Table 1

Sample	Rock (g)	M_{pyrite} (g)	Total (g)	Wt.% pyrite	Insolubles (g)	M_{lime} (g)	$\delta^{34}S_{app}$ ‰ VCDT	$[CAS]_{app}$ (ppm)	$[SO_4]_{pyrite}/[CAS]_{app}$
HClA	150.13	0	150.13	0	18.7	131	34.39	564	0
HClB	148.58	1.54	150.12	1.03	20.3	130	33.33	634	0.100
HClC	142.58	7.52	150.10	5.01	24.7	125	29.90	755	0.208
HClD	135.16	15.01	150.17	10.0	31.1	119	27.58	864	0.266
AceticA	150.05	0	150.05	0	27.8	122	34.98	539	0
AceticB	148.50	1.54	150.04	1.03	28.3	122	33.68	609	0.103
AceticC	142.53	7.53	150.06	5.02	31.0	119	29.55	761	0.246
AceticD	135.02	15.01	150.03	10.0	34.4	116	26.80	890	0.316

eight hours, and then filtered through a membrane filter (0.45 μm) to remove insoluble particulate matter.

An aliquot of 50 ml of a 30% $BaCl_2$ solution (300 g of anhydrous $BaCl_2$ powder dissolved into 1000 ml of DDI) was then added to each sample after heating to sub-boiling to precipitate $BaSO_4$. The samples were left for three days to ensure complete precipitation. The barite was then collected by filtration on a membrane filter (0.45 μm), which was then dried and weighed.

Filters containing insolubles were rinsed with multiple volumes of DDI before drying and weighing to remove residual acid. The starting sample mass less the mass of insolubles was used along with the mass of barite precipitated to determine CAS concentration.

2.3. Isotopic analysis of sulfur

A Eurovector elemental analyzer (EA) was used for on-line combustion of barite or pyrite and the separation of SO_2, interfaced with a Micromass Isoprime mass spectrometer for $^{34}S/^{32}S$ analyses. The effluent from the EA is introduced in a flow of He (80–120 ml/min) to the IRMS through a SGE splitter valve that controls the variable open split. Timed pulses of SO_2 reference gas (99.9% purity, ~3 nA) are introduced at the beginning of the run using an injector connected to the IRMS with a fixed open ratio split. The isotope ratios of reference and sample peaks are determined by monitoring ion beam intensities relative to background values.

Prepared samples (~100 μgrams for barite, ~50 μgrams for pyrite) are accurately weighed in duplicate and folded into small tin cups that are sequentially dropped with a pulsed O_2 purge of 12 ml into a catalytic combustion furnace operating at 1030 °C. The frosted quartz reaction tube is packed with granular tungstic oxide on alumina ($WO_3+Al_2O_3$) and high purity reduced copper wire for quantitative oxidation and O_2 resorption. Water is removed from the combustion products with a 10-cm magnesium perchlorate column, and the SO_2 is separated from other gases with a 0.8-m PTFE GC column packed with Porapak 50–80 mesh heated to 90 °C. The cycle time for these analyses was 210 s with reference gas injection as a 30-s pulse beginning at 20 s. Sample SO_2 pulses begin at 110 s and return to baseline values between 150 and 180 s, depending on sample size and column conditions. Isotope ratios are determined by comparing integrated peak areas of m/z 66 and 64 for the reference and sample SO_2 pulses, relative to the baseline of $\sim 1\times10^{-11}$ A. Isotopic results are expressed in the δ notation as per mil (‰) deviations from the VCDT standard (isotopic results from previous studies that were reported relative to the equivalent CDT standard, the original Canyon Diablo Troilite, are herein reported relative to CDT.) Uncertainties of these measurements (better than ±0.3‰) were determined by multiple analysis of a standard barite (NBS 127) interspersed with the samples.

3. Results

The pyrite used in this study yielded a $\delta^{34}S$ value of +9.39 ‰ (this value will be referred to as $\delta^{34}S_{pyrite}$). For the following discussion, sulfate resulting from the CAS extraction process will be referred to as 'apparent CAS'; its isotopic composition will be called $\delta^{34}S_{app}$ and its concentration will be $[CAS]_{app}$. The average apparent CAS concentration of the two unspiked samples are taken to represent the actual sulfate concentration in the original limestone sample ($[SO_4]_{lime}$=552 ppm). The two unspiked samples exhibit a standard deviation of 18 ppm, thus we regard the uncertainty in the $[CAS]_{app}$ measurements to be ~3%. Although the samples extracted using acetic acid resulted in a greater abundance of insolubles (18% of total starting mass vs. 12% for HCL), the $[CAS]_{app}$ values were similar to those extracted using HCl (Table 1), implying that the additional insolubles were un-reacted limestone. The isotopic compositions of the two unspiked samples are assumed to be that of the original limestone sample ($\delta^{34}S_{lime}$). The average $\delta^{34}S$ value of the unspiked samples is +34.7 ‰ (standard deviation=0.4‰, n=4 including one replicate for each).

For the following discussion, the mass of pyrite (M_{pyrite}) relative to the starting sample mass will be referred to as 'weight percent pyrite' whereas the mass of pyrite relative to the mass of limestone dissolved (M_{lime}, the starting sample mass minus insolubles) will be referred to as 'normalized fraction pyrite'. This distinction is made to facilitate the discussion of two-component mixing (see below), which assumes that only pyrite and limestone (not insolubles) contributed to the amount of sulfate extracted from the starting sample. The data reveal a positive correlation between apparent CAS concentration and weight percent pyrite (Fig. 1) for both acid treatments. Likewise, there is a distinct negative relationship between weight percent pyrite and $\delta^{34}S_{app}$ (Fig. 2). The correlations in Figs. 1 and 2 appear to be gently curved, but both correlations can be approximated via linear regression with high R^2 values (Figs. 1–2).

The apparent CAS concentration can be modeled according to the linear equation:

$$[CAS]_{app} = [SO_4]_{lime} + [SO_4]_{pyrite}$$

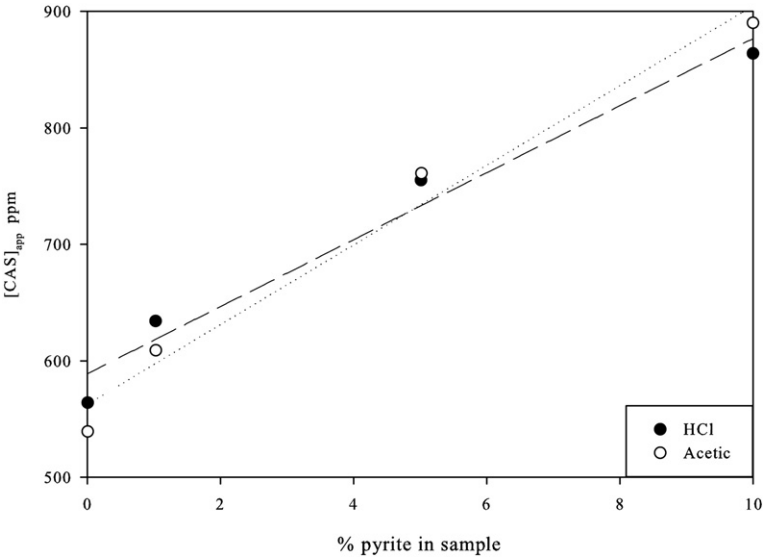

Fig. 1. Plot of sulfate concentration from CAS extraction versus weight percent pyrite. Long-dashed line is a linear regression through the HCl data with an R^2 of 0.9716. The short-dashed line is a linear regression through the acetic data with an R^2 of 0.9783.

$[SO_4]_{pyrite}$ is the concentration of sulfate resulting from the oxidation of pyrite and is related to the mass of pyrite according to:

$$[SO_4]_{pyrite} = w\frac{M_{pyrite}}{M_{lime}}$$

where w represents the ppm sulfate formed per gram pyrite, assuming that the amount of sulfate oxidized from pyrite is significant enough to affect $[CAS]_{app}$, but is insignificant compared to the mass of insolubles. The linear equation then becomes:

$$[CAS]_{app} = [SO_4]_{lime} + w\left(\frac{M_{pyrite}}{M_{lime}}\right)$$

so that on a plot of $[CAS]_{app}$ vs normalized mass pyrite, w can be determined from the slope of the line (Fig. 3).

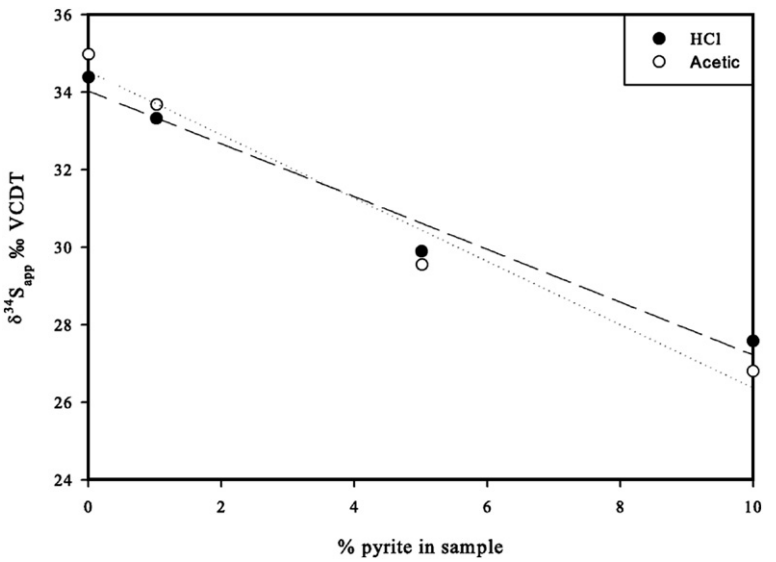

Fig. 2. Plot of $\delta^{34}S$ results from CAS extraction versus weight percent pyrite. The long-dashed line is a linear regression through the HCl data with an R^2 of 0.9736. The short-dashed line is a linear regression through the acetic data with an R^2 of 0.9727.

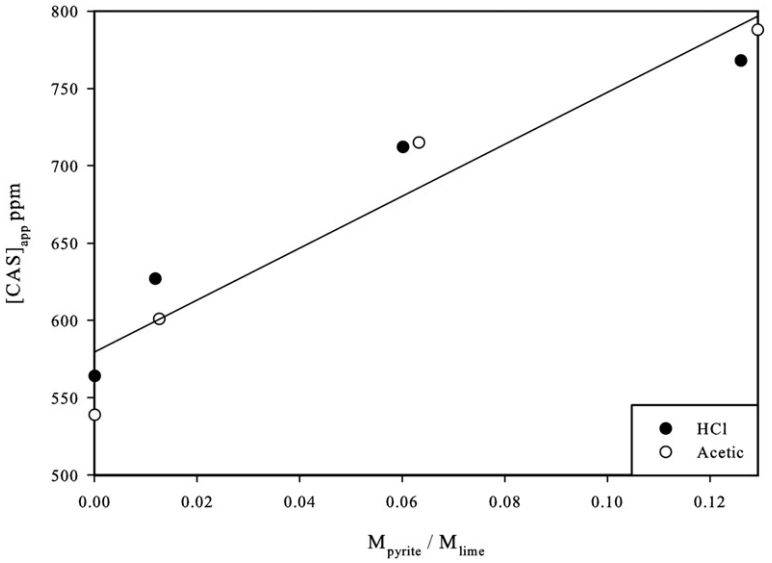

Fig. 3. Plot of modeled $[CAS]_{app}$ values versus the M_{pyrite}/M_{lime} values from this study. The line is fit through the entire data set (both HCl and acetic, $R^2=0.9129$, standard error=205.1 ppm).

A linear regression through the entire data set gives a slope of 1679±205 ppm ($R^2=0.9129$).

Likewise, the isotopic composition of apparent CAS can be modeled by treating it as a mixture of two components:

$$\delta^{34}S_{app} = \left(1 - \frac{[SO_4]_{pyrite}}{[CAS]_{app}}\right)\delta^{34}S_{lime} + \left(\frac{[SO_4]_{pyrite}}{[CAS]_{app}}\right)\delta^{34}S_{pyrite}$$

which can be simplified to:

$$\delta^{34}S_{app} = \left(\delta^{34}S_{pyrite} - \delta^{34}S_{lime}\right)\left(\frac{[SO_4]_{pyrite}}{[CAS]_{app}}\right) + \delta^{34}S_{lime}$$

Fig. 4 shows the plot of $\delta^{34}S_{app}$ versus $[SO_4]_{pyrite}/[CAS]_{app}$ for the samples in this study. A linear regression fit through the entire data set has an intercept that yields $\delta^{34}S_{pyrite}=+8.9‰$, quite similar to the measured $\delta^{34}S$ composition of the pyrite used in this study (+9.4‰), suggesting that little to no fractionation of sulfur occurred during the chemical oxidation of pyrite. The slope of the regression should yield $\delta^{34}S_{pyrite}-\delta^{34}S_{lime}$. The observed result is −25.7±2.4 ‰ ($R^2=0.9494$), quite similar to the result expected from the end-member compositions (=34.7−9.4=25.3‰).

4. Pyrite sulfide oxidation mechanisms

A number of studies have investigated the dissolution of pyrite in acidic solutions (e.g., Garrels and Thompson, 1960; Smith and Shumate, 1970; Hamilton and Woods, 1980; Nordstrom, 1982; Wiersma and Rimstidt, 1984; McKibben and Barnes, 1986; Buckley and Woods, 1987; Luther, 1987; Moses et al., 1987; Luther, 1990; Rimstidt and Newcomb, 1993; Sasaki, 1994; Sasaki et al., 1995; Rickard and Morse, 2005). Dissolution of pyrite can occur via oxidation by dissolved O_2 or by Fe^{3+} via the following overall reactions through a series of intermediate steps (e.g., Luther, 1987; Moses et al., 1987; Luther, 1990):

$$FeS_{2(s)} + \frac{7}{2}O_{2(aq)} + H_2O \rightarrow Fe^{2+} + 2SO_4^{2-} + 2H^+ \quad (1)$$

$$FeS_{2(s)} + 14Fe^{3+} + 8H_2O \rightarrow 15Fe^{2+} + 2SO_4^{2-} + 16H^+ \quad (2)$$

Moses et al. (1987) empirically determined that the rate of reaction for equation 2 is at least two orders of magnitude faster than that of reaction 1 at low pH, and one order of magnitude faster at high pH. Luther (1987, 1990) has discussed the reasons for the higher rates of reaction between pyrite and Fe^{3+} based on frontier-molecular-orbital theory. Because the rate of reaction 2 is considerably higher than that of reaction 1, it is likely that reaction 2 is the dominant mechanism for dissolving pyrite during CAS extraction. However a controlled analysis of O_2, H_2O and CAS $\delta^{18}O$ is needed to quantify the relative contribution of Fe^{3+} and O_2 pyrite oxidation, as some experiments have shown that pyrite oxidation by O_2 can be a significant component in certain systems (e.g., acid mine drainage, Earnest, 2002).

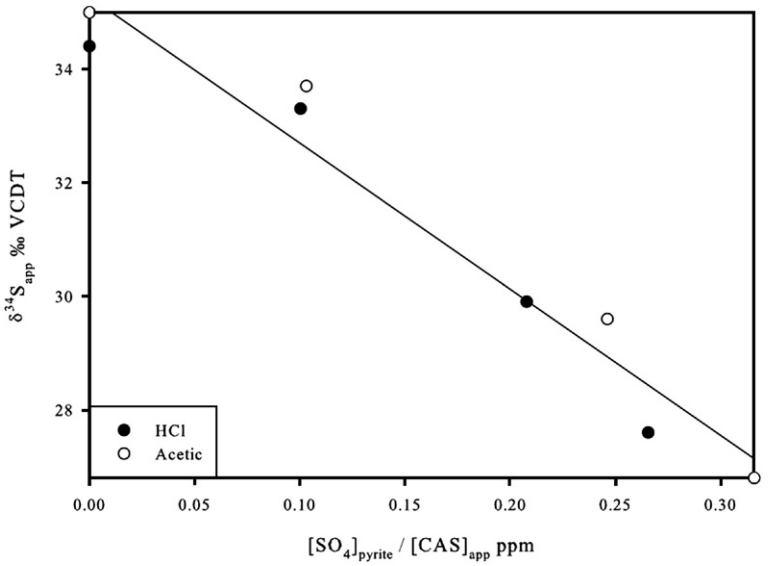

Fig. 4. Plot of modeled $\delta^{34}S_{app}$ values versus $[SO_4]_{pyrite}/[CAS]_{app}$ values from this study. The line is fit through the entire data set and has a slope of −25.7‰ (R^2=0.9494, standard error=2.4‰).

Dissolution of pyrite by Fe^{3+} has significant implications for the study of CAS. Carbonates are likely to contain significant amounts of detrital material that may contain reactive iron, most likely in the form of clay minerals and iron oxides. For example, the limestone used in this study came from the Virgin Limestone Member at Beyond Lost Cabin, where limestones have been reported to contain between 1200 and 3100 ppm Fe (Marenco, 2007). When CAS samples are acidified with HCl, reactive Fe may be liberated from clay minerals or iron oxides and subsequently react with FeS_2. Because the oxygen used to form the final SO_4^{2-} in reaction 2 is derived from H_2O, not from dissolved O_2, CAS extraction under anaerobic conditions might not prevent the oxidation of pyrite sulfide. However, Fe^{3+} can be re-supplied to the system via the reaction:

$$Fe^{2+} + \frac{1}{4}O_{2(aq)} + H^{+} \rightarrow Fe^{3+} + \frac{1}{2}H_2O \qquad (3)$$

which is known to limit the rate of pyrite dissolution at low pH (Moses et al., 1987). Therefore, extraction of CAS under anaerobic conditions may slow down but not prevent the dissolution of pyrite. A further implication of this process is that, because the oxygen in SO_4^{2-} in reaction 2 is derived from the water, not from the atmosphere, studies of $\delta^{18}O_{CAS}$ might be compromised, even if performed under anaerobic conditions.

The large difference between the rates of reactions 1 and 2 may explain the slight yet distinct curvature observed in Figs. 1–3. The Fe^{3+} supply to reaction 2 is sourced from the powdered limestone sample. However, in order to increase weight percent pyrite in our samples, the amount of limestone powder in a sample was decreased as the mass of pyrite was increased. Consequently, the samples with higher weight percent pyrite had less Fe^{3+} to begin with, and as such, dissolution by O_2 may have had an increased effect relative to dissolution by Fe^{3+}, leading to a slight but noticeable decrease in the percentage of pyrite oxidized to sulfate (Fig. 1).

Luther (1987, 1990) and Luther et al. (1997) have discussed the production of intermediate sulfur phases such as thiosulfate before the ultimate production of sulfate. However, at low pH, Moses et al. (1987) found no measurable sulfur intermediates when Fe^{3+} was used as an oxidant, but found that intermediates were significant when O_2 was the oxidant. The lack of observable intermediates in those studies was likely due to the reactivity of sulfur intermediates with H^+ and Fe^{3+} at low pH values (Williamson and Rimstidt, 1993; Luther et al., 1997).

The majority of the observed increase in sulfate during the Moses et al. (1987) experiment occurred during the first two hours. During CAS extraction, samples are commonly left dissolving for multiple hours (e.g., this study) to allow for the complete dissolution of $CaCO_3$, although this procedural variable is often omitted from published methods. After the dissolution step, a series of filtration steps, culminating in a 0.45 μm filtration, are performed in order to remove insolubles. Depending on the amount of insolubles, the combined filtration steps may add multiple hours to the amount of time that Fe^{3+} has to react with pyrite before the mineral

is isolated from the solution. Decreasing the amount of time for the initial acidification step, combined with techniques to speed up the filtrations (such as centrifuging the particulates down before filtering), may help to reduce the effect of pyrite dissolution on the resultant CAS data.

We have observed that many CAS samples exhibit a yellow fluid color after the acidification step, especially in samples with high amounts of insolubles. The yellow color, which does not disappear upon filtration through a 0.45 μm membrane, is likely due to the presence of dissolved or colloidal ferric iron released from the treated sample (Hurtgen et al., 2002). If this interpretation is correct, then a preliminary dissolution of a smaller sample size may be useful to determine if the sample contains abundant reactive Fe. Quantifying total Fe and pyrite abundance is crucial to determine which samples are susceptible to pyrite oxidation. The insoluble residue from a small sample could be subjected to a bulk sulfur analysis to assess its pyrite content.

5. Implications for future CAS studies

The results reported here provide conclusive evidence that pyrite is oxidized by either hydrochloric or acetic acid during the extraction of CAS. Our findings have significant implications for the future use of CAS to study ancient seawater sulfate. As a minimum, studies of CAS should include some attempt to quantify pyrite abundance and Fe abundance in samples. With only 1% pyrite with a $\delta^{34}S$ composition of +9 ‰, an isotopic depletion of >1‰ was observed relative to the true value of CAS in the sample of ~+38‰. Because pyrite in sedimentary rocks can exhibit much lower $\delta^{34}S$ values (down to −50‰ or greater, Hoefs, 1997), the isotopic influence of pyrite in this study are small compared to the range of possible values. Using the slope of the line in Fig. 3, we can predict the effects of pyrite with different $\delta^{34}S$ compositions on $[CAS]_{app}$ and $\delta^{34}S_{app}$. Fig. 5 shows a plot of $[CAS]_{app}$ and $\delta^{34}S_{app}-\delta^{34}S_{lime}$ at various compositions of $\delta^{34}S_{pyrite}$ (shown as $\Delta\delta=\delta^{34}S_{lime}-\delta^{34}S_{pyrite}$) versus the mass fraction pyrite. Even at low pyrite to limestone ratios, the oxidation of pyrite can have significant effects on the $\delta^{34}S$ of apparent CAS if the $\delta^{34}S$ composition of the pyrite is much less than that of the limestone. Realistically, limestones are unlikely to have more than 1 wt.% pyrite (e.g., Riccardi et al., 2006). Therefore it should be noted that with a large $\Delta\delta$ (e.g., $\Delta\delta=70$ in Fig. 5), a sample with a normalized fraction pyrite of 1% or less exhibits a maximum isotopic offset of about −4‰, and a $[CAS]_{app}$ offset of about 17 ppm. Consequently, in samples with much less than 1 wt.% pyrite and $\Delta\delta$ values much lower than 70, it can be argued that the isotopic effect of any pyrite oxidized would be much less than −4‰. However, naturally-occurring pyrite is likely to be much finer-grained than the pyrite used in this study. Because rates of pyrite dissolution increase as grain size decreases (e.g., Sasaki, 1994), the isotopic offsets from naturally-occurring pyrite might be larger than those reported here. Likewise, in samples with much lower [CAS], the effect of pyrite oxidation would be much larger.

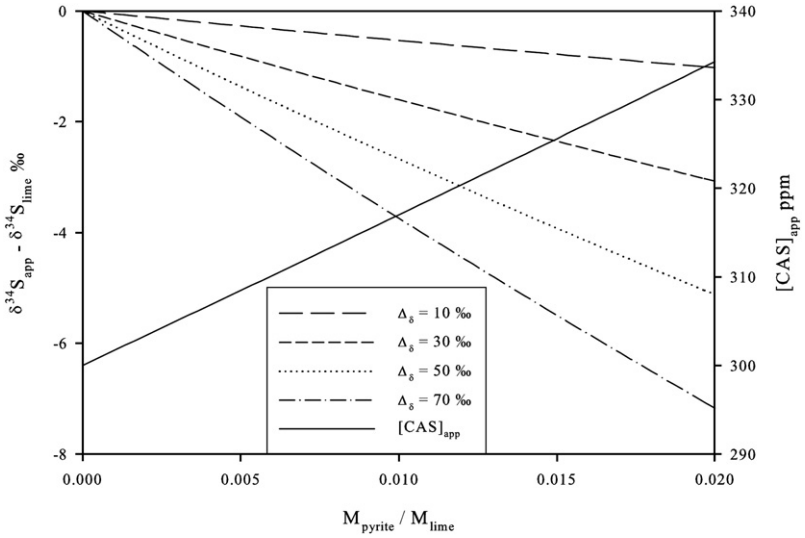

Fig. 5. Results of modeling using the slope of the line in Fig. 3 with a hypothetical $[SO_4]_{lime}$ of 300 ppm and different $\delta^{34}S_{pyrite}$ values. The left-hand axis shows the difference between the $\delta^{34}S$ of apparent CAS and limestone, assuming that the difference between the $\delta^{34}S$ of limestone and pyrite ($\Delta\delta$) are either 10, 30, 50, or 70 ‰. The right-hand axis shows the concentration of apparent CAS. Both plots are given relative to M_{pyrite}/M_{lime}.

There is a possibility that sedimentary pyrite may be oxidized during diagenesis via the mechanisms discussed here (e.g., Riccardi et al., 2006). However, the diagenetic incorporation of sulfate into limestones is poorly understood and warrants further investigation. Therefore, we would recommend that samples with abundant pyrite or pyrite pseudomorphs should be avoided for CAS analysis. Based on our results and mixing models, and assuming highly depleted $\delta^{34}S$ values and smaller grain sizes for natural pyrite, even samples with 1 wt.% pyrite or less can be influenced by up to a few permil. If pyrite is present, it is likely that the availability of reactive Fe is the dominant control on whether it is oxidized during CAS extraction.

Acknowledgements

This project was supported by NSF (EAR 0447019) to Corsetti, Bottjer and Kaufman. Marenco was additionally supported with graduate student grants from the Geological Society of America, the American Association of Petroleum Geologists, the Paleontological Society, and USC Earth Sciences Department. The authors wish to express their gratitude to Tim Lyons and David Rickard for reviews that contributed significantly to the final version of this manuscript.

References

Blakey, R.C., 1974. Stratigraphic and depositional analysis of the Moenkopi Formation, Southeastern Utah. Bulletin- Utah Geological and Mineral Survey 104, 1–81.

Buckley, A.N., Woods, R., 1987. The surface oxidation of pyrite. Applications of Surface Science 27, 437–452.

Burdett, J.W., Arthur, M.A., Richardson, M., 1989. A Neogene seawater sulfur isotope age curve from calcareous pelagic microfossils. Earth and Planetary Science Letters 94 (3–4), 189–198.

Canfield, D.E., 1998. A new model for Proterozoic ocean chemistry. Nature 396 (6710), 450–453.

Claypool, G.E., Holser, W.T., Kaplan, I.R., Sakai, H., Zak, I., 1980. The age curves of sulfur and oxygen isotopes in marine sulfate and their mutual interpretation. Chemical Geology 28 (3–4), 199–260.

Earnest, D.J., 2002. Isotopic determination of water sources to and mechanisms of acid generation in acid mine drainage at the Kempton mine. Master's Thesis, University of Maryland, College Park, 82 pp.

Garrels, R.M., Thompson, M.E., 1960. Oxidation of pyrite by iron sulfate solutions. American Journal of Science 258-A, 57–67.

Gellatly, A.M., Lyons, T.W., 2005. Trace sulfate in mid-Proterozoic carbonates and the sulfur isotope record of biospheric evolution. Geochimica et Cosmochimica Acta 69 (15), 3813–3829.

Hamilton, I.C., Woods, R., 1980. An investigation of surface oxidation of pyrite and pyrrhotite by linear potential sweep voltammetry. Journal of Electroanalytical Chemistry 118, 327–343.

Hoefs, J., 1997. Stable Isotope Geochemistry. Springer-Verlag. 201 pp.

Holser, W.T., 1984. Gradual and abrupt shifts in ocean chemistry during Phanerozoic time. In: Holland, H.D., Trendall, A.F. (Eds.), Patterns of change in Earth evolution. Springer-Verlag, Berlin, pp. 123–143.

Hurtgen, M.T., Arthur, M.A., Suits, N.S., Kaufman, A.J., 2002. The sulfur isotopic composition of Neoproterozoic seawater sulfate; implications for a snowball Earth? Earth and Planetary Science Letters 203 (1), 413–429.

Kah, L.C., Lyons, T.W., Frank, T.D., 2004. Low marine sulphate and protracted oxygenation of the Proterozoic biosphere. Nature 431, 834–837.

Kaiho, K., Chen, Z.-Q., Kawahata, H., Kajiwara, Y., Sato, H., 2006. Close-up of the end-Permian mass extinction horizon recorded in the Meishan section, South China: sedimentary, elemental, and biotic characterization and a negative shift of sulfate sulfur isotope ratio. Palaeogeography, Palaeoclimatology, Palaeoecology 239, 396–405.

Kaiho, K., et al., 2001. End-Permian catastrophe by a bolide impact; evidence of a gigantic release of sulfur from the mantle. Geology 29 (9), 815–818.

Kampschulte, A., Strauss, H., 2004. The sulfur isotopic evolution of Phanerozoic seawater based on the analysis of structurally substituted sulfate in carbonates. Chemical Geology 204, 255–286.

Kaplan, I.R., Emery, K.O., Rittenberg, S.C., 1963. The distribution and isotopic abundance of sulphur in recent marine sediments off southern California. Geochimica et Cosmochimica Acta 27 (4), 297–331.

Luther III, G.W., 1987. Pyrite oxidation and reduction; molecular orbital theory considerations. Geochimica et Cosmochimica Acta 51 (12), 3193–3199.

Luther III, G.W., 1990. The frontier-molecular-orbital theory approach in geochemical processes. In: Stumm, W. (Ed.), Aquatic chemical kinetics; reaction rates of processes in natural waters. W. John and Sons, New York, NY, pp. 173–198.

Luther III, G.W., Sasaki, K., Tsunekawa, M., Ohtsuka, T., Konno, H., 1997. Confirmation of a sulfur-rich layer on pyrite after oxidative dissolution by Fe(III) ions around pH 2; discussion and reply. Geochimica et Cosmochimica Acta 61 (15), 3269–3274.

Lyons, T.W., Walter, L.M., Gellatly, A.M., Marini, A.M., 2004. Sites of anomalous organic remineralization in the carbonate sediments of South Florida, U.S.A.: the sulfur cycle and carbonate-associated sulfate. In: Amend, J., Edwards, K., L.T. (Eds.), Microbial Sulfur Transformations Throughout Earth's History: Development, Changes, and Future of the Biogeochemical Sulfur Cycle: Geological Society of America Special Paper 379. Geological Society of America, Boulder, pp. 161–176.

Marenco, P.J., 2007. Sulfur isotope geochemistry and the End Permian mass extinction. Dissertation Thesis, University of Southern California, Los Angeles, 189 pp.

McKee, E.D., 1954. Stratigraphy and history of the Moenkopi Formation of Triassic age. Geological Society of America (GSA). Boulder, CO. 133 pp.

McKibben, M.A., Barnes, H.L., 1986. Oxidation of pyrite in low temperature acidic solutions; rate laws and surface textures. Geochimica et Cosmochimica Acta 50 (7), 1509–1520.

Mekhtiyeva, V.L., 1974. Sulfur isotopic composition of fossil molluscan shells as an indicator of hydrochemical conditions in ancient basins. Geochemistry International 11 (6), 1188–1192.

Moses, C.O., Nordstrom, D.K., Herman, J.S., Mills, A.L., 1987. Aqueous pyrite oxidation by dissolved oxygen and by ferric iron. Geochimica et Cosmochimica Acta 51 (6), 1561–1571.

Newton, R., Pevitt, P., Wignall, P.B., Bottrell, S., 2004. Large shifts in the isotopic composition of seawater sulphate across the Permo-

Triassic boundary in northern Italy. Earth and Planetary Science Letters 218, 331–345.

Nordstrom, D.K., 1982. Aqueous pyrite oxidation and the consequent formation of secondary iron minerals. In: Kittrick, J.A., Fanning, D.S., Hossner, L.R., Kral, D.M., Hawkins, S. (Eds.), Acid sulfate weathering. Soil Science Society of America, pp. 37–56.

Riccardi, A.L., Arthur, M.A., Kump, L.R., 2006. Sulfur isotopic evidence for chemocline upward excursions during the end-Permian mass extinction. Geochimica et Cosmochimica Acta 70, 5740–5752.

Rickard, D., Morse, J.W., 2005. Acid volatile sulfide (AVS). Marine Chemistry 97 (3–4), 141–197.

Rimstidt, J.D., Newcomb, W.D., 1993. Measurement and analysis of rate data; the rate of reaction of ferric iron with pyrite. Geochimica et Cosmochimica Acta 57 (9), 1919–1934.

Sasaki, K., 1994. Effect of grinding on the rate of oxidation of pyrite by oxygen in acid solutions. Geochimica et Cosmochimica Acta 58 (21), 4649–4655.

Sasaki, K., Tsunekawa, M., Ohtsuka, T., Konno, H., 1995. Confirmation of a sulfur-rich layer on pyrite after oxidative dissolution by Fe(III) ions around pH 2. Geochimica et Cosmochimica Acta 59 (15), 3155–3158.

Smith, E.E., Shumate, K.S., 1970. Sulfide to sulfate reaction mechanism; a study of the sulfide to sulfate reaction mechanism as it relates to the formation of acid mine waters. 115 pp.

Wiersma, C.L., Rimstidt, J.D., 1984. Rates of reaction of pyrite and marcasite with ferric iron at pH 2. Geochimica et Cosmochimica Acta 48 (1), 85–92.

Wilgus, C.K., 1981. A stable isotope study of Permian and Triassic marine evaporite and carbonate rocks, Western Interior, U.S.A. Doctoral Thesis, University of Oregon, Eugene, OR, 109 pp.

Williamson, M.A., Rimstidt, J.D., 1993. The rate of decomposition of the ferric-thiosulfate complex in acidic aqueous solutions. Geochimica et Cosmochimica Acta 57 (15), 3555–3561.